Paper

THE USE OF FDTD IN ESTABLISHING IN VITRO EXPERIMENTATION CONDITIONS REPRESENTATIVE OF LIFELIKE CELL PHONE RADIATION ON THE SPERMATOZOA

Rand Mouradi,*† Nisarg Desai,*‡ Ahmet Erdemir,§ and Ashok Agarwal*

Abstract—**Recent studies have shown that exposing human semen samples to cell phone radiation leads to a significant decline in sperm parameters. In daily living, a cell phone is usually kept in proximity to the groin, such as in a trouser pocket, separated from the testes by multiple layers of tissue. The aim of this study was to calculate the distance between cell phone and semen sample to set up an in vitro experiment that can mimic real life conditions (cell phone in trouser pocket separated by multiple tissue layers). For this reason, a computational model of scrotal tissues was designed by considering these separating layers, the results of which were used in a series of simulations using the Finite Difference Time Domain (FDTD) method. To provide an equivalent effect of multiple tissue layers, these results showed that the distance between a cell phone and semen sample should be 0.8 cm to 1.8 cm greater than the anticipated distance between a cell phone and the testes.**

Health Phys. 102(1):54–62; 2012

Key words: dosimetry; electromagnetic fields; exposure, radiation; radiation effects

INTRODUCTION

THE RAPID growth of cell phone use during the last decade has led to various health concerns (WHO 2006; Blank and Goodman 2008; Makker et al. 2009). Among these concerns, the effect of radiofrequency electromagnetic waves (RF-EMW) on male fertility has drawn much attention (Agarwal et al. 2008, 2009). According to epidemiological studies performed in the last decade, a decline in male infertility seen recently in developed nations might be related in part to cell phone use (Davoudi et al. 2002; Fejes et al. 2005; Wdowiak et al. 2007; Agarwal et al. 2008, 2009). A published in vitro study from this laboratory supports that theory. The current results showed that even as little as 1 h of exposure to RF-EMW led to an increase in ROS (Reactive Oxygen Species) levels in semen samples, which in turn caused oxidative stress to occur (Agarwal et al. 2008, 2009). Moreover, these increased levels of ROS were linked to a decline in sperm parameters when semen samples were kept 2.5 cm from a cell phone.

It is difficult to accurately estimate the amount of RF-EMW the human testes are exposed to during a cell phone call because they are protected by multiple layers of tissue in the scrotum. In addition, the amount of exposure depends on the location of the radiation source. Many men carry their cell phone (on talk mode) close to the groin, in a trouser pocket for example, or clipped to a belt on their waist, while using an ear piece (Bluetooth) to handle their calls. This technology exposes the testes to a higher amount of radiation than a cell phone in the "stand by mode" in a trouser pocket. Therefore, a more realistic approach is needed to quantify the effects of RF-EMW on the male reproductive system.

Computational RF dosimetry has been used by previous researchers to calculate the amount of RF energy deposited in the "head of the user" (Beard and Kainz 2004; Christ et al. 2006). Specifically, computational simulation has been used to estimate the amount of RF energy and specific absorbance rate (SAR) deposition in the heads of cell phone users. However, no study has reported on the use of the computational approach to study effects of RF-EMW on spermatozoa. Furthermore, there are no available guidelines in the literature for the setup of in vitro studies to mimic real-life conditions (Fig. 1).

This study was conducted, therefore, to establish guidelines for future in vitro studies on human semen. It is anticipated that this equivalent distance will replicate the real life conditions of men who carry cellular phones

* Center for Reproductive Medicine, Glickman Urological and Kidney Institute and Obstetrics and Gynecology and Women's Health Institute, Cleveland Clinic, Cleveland, OH; † Department of Electrical and Computer Engineering, Cleveland State University, OH; ‡ Department of Internal Medicine, Staten Island University Hospital, New York, NY; § Computational Biomodeling (CoBi) Core, Department of Biomedical Engineering, Lerner Research Institute, Cleveland Clinic, Cleveland, OH.

Ahmet Erdemir has equity in Innodof LLC; the other authors declare no conflict of interest

For correspondence contact: Ashok Agarwal, Center for Reproductive Medicine, Cleveland Clinic, 9500 Euclid Avenue, Desk A19.1, Cleveland, OH 44195, or email at agarwaa@ccf.org.

(*Manuscript accepted* 14 *June* 2011)
0017-9078//0

DOI: 10.1097/HP.0b013e3182289bfb

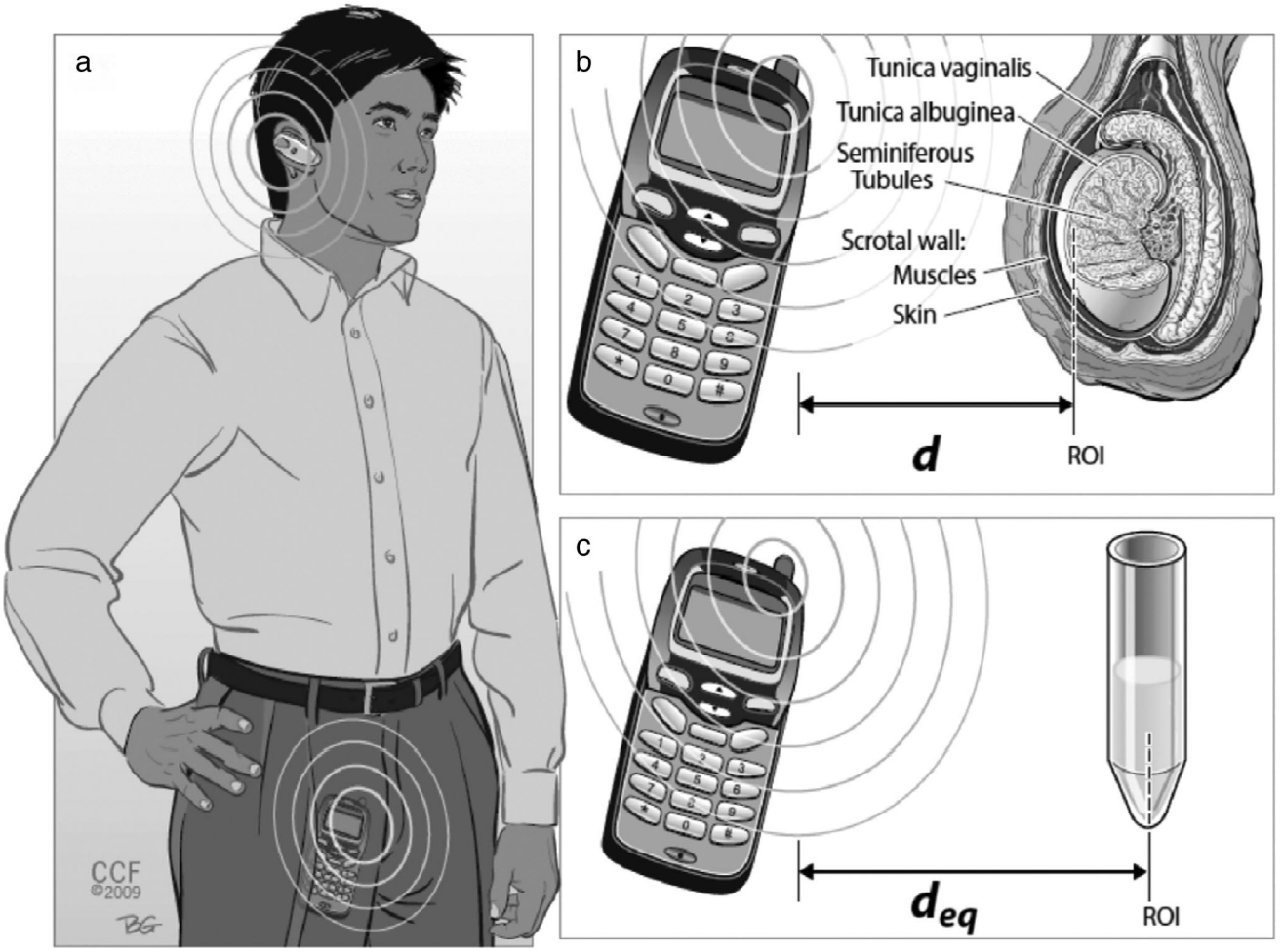

Fig. 1. (a) A man having a cell phone conversation via an ear piece while holding the phone handset in his pocket close to his reproductive organs; (b) an anatomical model for the basic testicular tissue layers with the cell phone located at a distance, d, from it; (c) the experimental setup of a semen sample in a test tube and the cell phone at an equivalent distance, d_{eq}, from the tube.

near their reproductive organs. For different real life situations (e.g., cell phone in a pocket or at the belt), a range of in vitro testing setups can be established by adjusting the distance between the cell phone and a test tube (used to represent the semen sample). Note that the Bluetooth radiation emitted from the earpiece during a call was ignored due to the large distance between the ear and genitals and the fact that the radiation emitted from the Bluetooth is much less than that of the cell phone (Karygiannis et al. 2002).

Aims and objectives

1. To define the models that represent testicular tissue and the cell phone radiation source (Fig. 1b);
2. To define the models representing the in vitro experiment with the source being in the air medium and the sample within the test tube (Fig. 1c);
3. To define the region of interest (ROI) in both models where the energy was compared;
4. To calculate the energy distribution for all models where the source was placed at different distances from the outermost layer in each model; and
5. To calculate and compare the mean values of energy density at the ROI in an anatomical model and in vitro model to establish the relationship between the range of distances in the tissue model and its corresponding range of equivalent distances in an in vitro experimental setting.

The results would relate the effects found in a previous experimental work (Agarwal et al. 2008, 2009) to a realistic cell phone usage scenario.

MATERIALS AND METHODS

The study was approved by the Cleveland Clinic Institutional Review Board. The study was completed in steps as follows.

The anatomical lifelike model

A two-dimensional model of the testicular region was developed to represent the tissue layers in the scrotum consisting of integument, dartos, external spermatic fascia, cremaster, infundibular fascia, tunica vaginalis, tunica albugenia, seminiferous tubules, and spermatozoa (Casey et al. 1982; Clemente 1985) (Fig. 1). Because the computer model was two-dimensional, only the thickness of the individual layers was represented and not the curvature of the scrotum. The range of tissue thicknesses for each of the tissue layers was obtained from the literature, and the most common values in an average adult male human were emphasized for comparison purposes. The scrotal wall thickness was commonly reported to be around 3 mm but can vary from 2 mm to 8 mm (Casey et al. 1982; Clemente 1985; Dogra et al. 2003; Standring 2004). The variation in the thickness of the scrotum depends on different conditions such as the surrounding temperature, and it also differs from one person to another (Dogra et al. 2003). The wall thickness of the seminiferous tubules was neglected since its thickness is considerably small (the whole diameter of a tubule is about 0.12 mm) compared to the other layers considered for modeling (Standring 2004). However, different tissue thicknesses were considered for a sensitivity analysis to test if they had any significant effect on the results (see section "Simulation Conditions").

The tunics layer is very thin and measures only about 0.1–0.2 mm according to Casey et al. (1982), while Copenhaver (1978) indicated that the tunica albuginea thickness is about 0.5 mm. The size of 0.5 mm was adopted for the basic simulation to account for the cavity of the tunica vaginalis and other small tissues of the septa between the tunica albuginea and the seminiferous tubules. The last layer was a fluid representing the spermatozoa and other cells inside the seminiferous tubules.

In vitro experimentation model

A two-dimensional model with the same computational cell size as the layered tissue model was developed to represent the cellular phone source. The resolution (size of computation cell) was dictated by a cell size of 0.05 cm for both models. A semen sample was placed in a test tube with the air medium filling the surroundings (Fig. 1). The test tube was a standard polystyrene test tube with a 16-mm diameter and a 1-mm wall thickness. Because the fluid sample was placed in the test tube, the fluid layer thickness was set to 16 mm to match the diameter of the test tube.

Region of interest (ROI) for computational models

The fluid layer thickness in both models was chosen as 16 mm to correspond to the diameter of the test tube for comparison purposes, and the region of interest (ROI) was positioned at the center of the fluid layer. Therefore, for the in vitro setup, the ROI was positioned at the center of the fluid layer that was 0.8 cm from the testing tube layer. Also, for comparison purposes, the ROI for the anatomical model was considered in the layer representing the spermatozoa at 0.8 cm from the inner layer of the model (tunica albugenia).

Calculating energy distribution by RF dosimetry

The finite difference time domain method (FDTD) has been used to calculate RF-EMW exposure in the human brain (Bit-Babik et al. 2003). Similarly, the amount of energy exposure to testicular tissues and spermatozoa caused by cell phone electromagnetic radiation can be predicted using this technique.

FDTD is a common computational technique used in electromagnetic applications to solve Maxwell's equations represented as partial differential equations (Taflove 2005). The technique relies on the discretization of the spatial and time domains by central difference approximations. Electrical and magnetic fields can be calculated at predesignated time points. The simulation then progresses and continues to the next time point until the final time is reached to terminate the simulation. Also, a current source was defined in the models to represent the electromagnetic effects of the cell phone. The geometries of the models were based on either the placement of a semen sample in a tube of known geometry or a layer of semen behind the tissue layers of the testicular region. The FDTD method quantifies the amount of energy density within a layer, and this is related to the specific absorption rate (SAR). The SAR is a major safety measure used to set a standardized limit for the amount of energy absorbed by body tissues. It is expressed in units of W kg^{-1} and is defined as (Barnes 2007):

$$SAR = \sigma |E|^2 \rho^{-1}, \quad (1)$$

where E is the electric field strength, a vector field (N/C or the equivalent units of V m^{-1}); σ is the conductivity of the medium (S m^{-1}); and ρ is the density of the tissue (kg m^{-3}).

SAR is commonly evaluated over a cubic volume, V, which contains a tissue mass of 1 g or 10 g (Bit-Babik et al. 2003):

$$SAR_v = [\int_v (\sigma |E|^2 / \rho) dV]/V. \quad (2)$$

Another important measure of exposure that is directly proportional to SAR is the electric field energy density, u, defined as

$$u = \frac{1}{2}\varepsilon|E|^2, \quad (3)$$

where ε is the dielectric constant or the permittivity of the material (Tretyakov 2005).

Because all of the dielectric parameters—ε, σ, and ρ—are constant for the same material under similar conditions, the only variable remaining in eqns (1), (2), and (3) is the electric field strength, E. Thus, for ease of comparison in this study, the electric field strength and the electric field energy density were the variables of interest to compare the energy distribution at the ROI.

To perform simulations using FDTD, this study used the open source software package Meep, MIT Electromagnetic Equation Propagation (ab-initio.mit.edu/wiki/index.php/Meep), which was developed for electromagnetic field simulations (Gajsek et al. 2001; Farjadpour et al. 2006). The predictions of the electric field in the models were post-processed using IPython (ipython.scipy.org/), an interactive Python programming environment using PyTables (www.pytables.org) to access Meep results stored in Hierarchical Data Format (HDF5); NumPy (numpy.scipy.org/) to perform matrix operations; and matplotlib (matplotlib.sourceforge.net/) for visualization. Based on the data generated by Meep, these tools were used to calculate the mean values of the energy density at the ROI and to illustrate the energy distribution throughout the models under all conditions considered for comparison. The final results for equivalent displacement calculations were conducted using OpenOffice.org Calc (www.openoffice.org/) and Excel (Microsoft Corp, Redmond, WA).

Dielectric parameters

The dielectric parameters (the relative permittivity, ε_r, and electrical conductivity, σ) for each layer were obtained from the literature (Gabriel et al. 1996; Christ et al. 2006) and using calculations provided by the Italian National Research Council, IFAC (niremf.ifac.cnr.it/tissprop/htmlclie/htmlclie.htm#stsftag) at 900 MHz and 1,800 MHz frequencies (Table 1). The dielectric parameters of semen at the specified frequencies were not found in the literature. However, since the water content of a biological tissue is the factor that has the most influence on its dielectric properties (Christ et al. 2006), it is likely that the choice of any body fluid would be adequate for comparison purposes, especially when the same type of fluid is used in all compared models. In this study, the dielectric properties of blood were used for the fluid layer to represent the semen layer in the experimental- and tissue-layered models. The dielectric parameters of the testis were used to represent the tunic layer. The air medium was selected to be the default medium that separated the cell phone source and the tissue layers and filled in the rest of the model.

Table 1. Dielectric parameters of the tissue layers at 900 MHz and 1,800 MHz. Note that the relative permittivity, ε_r, is unitless because it is normalized by the air permittivity.

Tissue Type	900 MHz		1,800 MHz	
	Permittivity, ε_r	Conductivity, σ (S/m)	Permittivity, ε_r	Conductivity, σ (S/m)
Skin	41.41	0.87	38.87	1.19
Muscle	56.90	1.00	55.30	1.44
Testicular tissues (tunics)	60.55	1.21	58.61	1.69
Fluid (blood)	61.40	1.54	59.37	2.04

The overall width and height of the modeled area were 200 mm and 300 mm, respectively. This size allowed the simulation of the electric field at the ROI without undesirable effects of the model boundaries. This computational domain size was calculated by gradually enlarging the domain of calculation until stable conditions were reached. At that point, no additional numerical change was noticed by further enlargement. This change in computational domain size was intended to eliminate any numerical disruption that might occur due to the proximity of the absorbing perfectly matched layers (PML) located at the computational cell boundaries (Laakso et al. 2007). In FDTD simulations, PML prevents reflection of electromagnetic waves.

The relative permittivity and conductivity of the polystyrene tube was found to be 2.56 (Yang 1996) and 1E-16 S/m (www.bistra.com.tr/deu_kimyacielkitabi.asp), respectively. For the semen layer, the same fluid dielectric parameters used in the layered tissue model were applied.

Simulation conditions

As explained in Fig. 2, the source was located at the center of the horizontal axis (x-axis) and at a certain distance from the outermost layer on the vertical axis (Y-axis) in each model. Simulations were conducted for two current source types representing the cell phone antenna—point (one-dimensional) and line (two-dimensional)—in order to compare the effect of antenna size on energy density distribution. To closely mimic a 3.5-cm loop antenna, which was used in this in vitro pilot study, the line source length was selected to be 3.5 cm on the x-axis. Two different frequencies were used to compare the energy densities generated by the frequency bands that are common in most parts of the world: 900 MHz and 1,800 MHz. The distance between the source and outermost layer (vertical) was varied between 0.5 cm and 9 cm in the tissue layer model and between 0.5 cm and 7.5 cm in the experimental setup model. Each simulation lasted for a 10-cycle duration of the electromagnetic field signals. For each

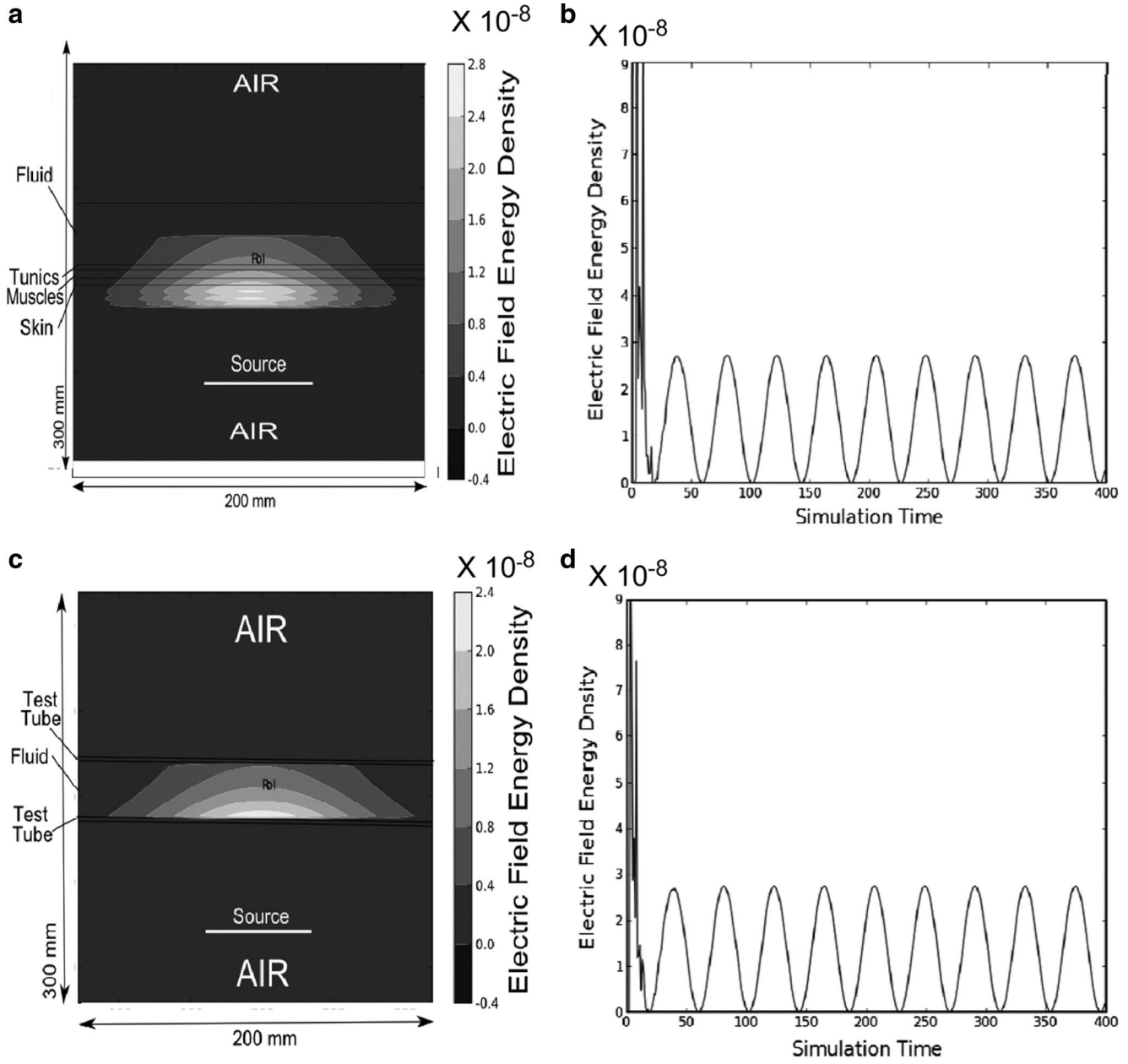

Fig. 2. (a) The energy density distribution through the basic lifelike model taken at a time instant representative of the mean values of electric field energy density with the 900 MHz line source 2.5 cm away from the outmost layer; (b) the time history of the electric field energy density at the ROI for the model in (a); (c) the energy density distribution through the basic lifelike model taken at a time instant representative of the mean values of the electric field energy density with the 900-MHz line source at 3.3 cm away from the tube layer; (d) the time history of electric field energy density at the ROI for the model in (c).

model and each simulation condition, the time history of the electromagnetic field distribution was calculated in addition to electric field energy density. In the ROI, the average of the electric field energy density during the simulations was also calculated over the steady state results. These values were used to find equivalent source locations between real life and in vitro experimentation conditions providing a similar average electromagnetic effect.

Sensitivity analysis

A sensitivity analysis was performed to estimate the influence of uncertainty in tissue thickness on the simulations. A point source at a frequency of 900 MHz

located 2.5 cm from the outermost tissue layer was used with varying tissue thickness values. A total of six models were developed. The distance between the source and the outmost layer was fixed at 2.5 cm. The scrotal wall thicknesses were varied from 2 mm to 8 mm, with the tunics tissues fixed at 0.2 mm. The tunics layer thickness was also tested at 0.2 mm and 0.5 mm, according to numbers reported in the literature (Casey et al. 1982) (Table 2). In each model, the mean value of the energy density in the ROI was calculated. Also, the size of the computational cell was decreased to make sure there were no artifacts due to discretization. This model was tested from 10–4,000 pixels m^{-1}, and after 2,000, there was no more change and a steady state was reached.

RESULTS

In Fig. 2a, the electric field energy density throughout the base layered tissue model is shown. In this simulation, a line source at 900 MHz was placed 2.5 cm from the scrotal skin layer (the thickness chosen for the scrotal wall was 3 mm, and the thickness chosen for the tunics area was 0.5 mm). The electric field energy density was higher for the regions closer to the source, as expected (Fig. 2).

Fig. 2b depicts the electric field energy density, u, at the ROI as a function of time. The waveform in this figure shows the highest values at the beginning of the time cycle followed by a steady sinusoidal waveform with a mean energy density of 1.44×10^{-8}. The results of Meep were normalized, so no unit was assigned for these values.

The electric field energy density distribution and the corresponding waveforms at the ROI are provided in Figs. 3a and b, respectively, for the experimental air-tube model. In this case, the source was positioned 3.3 cm from the first tube layer. The mean value of u calculated at the ROI for the latter model was 1.404×10^{-8}. The energy density values at the ROI of this experimental model were the closest match to the values at the ROI in the layered tissue model described in Fig. 2.

The two models were simulated for a range of source locations (distance from outermost tissue or tube boundary), and the mean values of the electric field energy densities were extracted in all cases. The mean values of the electric field energy density in the lifelike model at certain distances were matched with their equivalent values in the experimental model. For each matching energy density value in the experimental model, the corresponding equivalent distance in the lifelike model was noted. Based on this comparison, the line charts in Fig. 3 were constructed to illustrate these values and relate all distances tested in the layered tissue model to their corresponding equivalents in the experimental model.

The simulations were repeated with a point source replacing the line source to determine the effect of the antenna size on the energy density values. The energy density was significantly higher when a point source was used. While the absolute magnitudes of the electric field changed when using a point source instead of a line source, the relative relationship between electric fields predicted for the anatomical model and the in vivo conditions remained similar. Therefore, an equivalent distance obtained from point source simulations will likely apply under line source conditions.

A source with an 1,800 MHz frequency was used in place of the 900 MHz source for both models to evaluate the effect of this frequency band on the energy distribution in the ROI. The distance between the source and the outermost tissue layer was fixed at 2.5 cm for the lifelike model. The simulation result of this model resulted in a mean average electric field energy density, u, at the ROI of 1.897×10^{-8}. The closest match between the experimental model at 1,800 MHz and the lifelike model occurred when the source was 3.3 cm from the tube layer, which had an amount of energy density that averaged 1.809×10^{-8} at the ROI.

DISCUSSION AND CONCLUSION

In the present study, the relationship between an in vitro experimental setup and real life conditions was established where men conduct cell phone conversations

Table 2. Layered tissue models tested with different thicknesses with the radiation source 2.5 cm from the outmost layer. Model 3 is the base layered tissue model selected for major simulations.

Model	Scrotum thickness Skin/ Muscle (mm)		Tunics tissues (mm)	Normalized mean of Electric field energy density ($\times 10^{-8}$)	Equivalent distance in experiment model (cm)
1	1	1	0.2	1.46	3.2
2	2	1	0.2	1.40	3.3
3	2	1	0.5	1.44	3.3
4	4	3	0.2	1.24	4.0
5	4	4	0.2	1.09	4.3
6	6	2	0.2	1.13	4.3

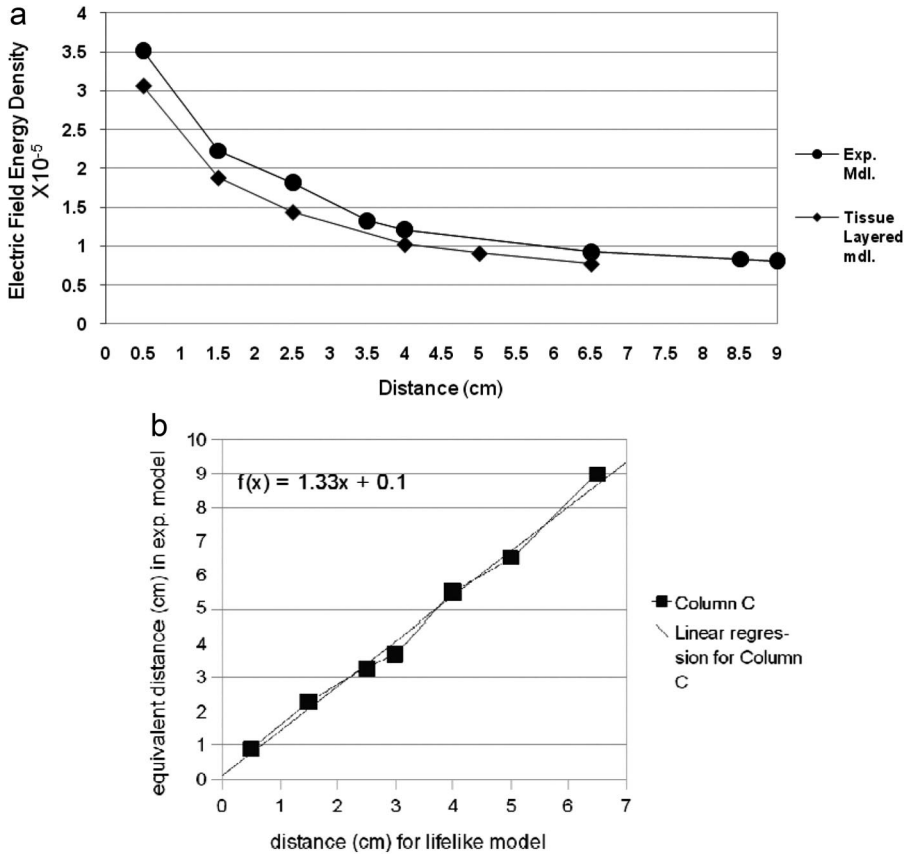

Fig. 3. (a) The average values of the electric field energy density at the ROI for the layered tissue model and for the in vitro experimentation model as a function of distance between the source and outermost region of the model. A 900-MHz line source was used for this simulation. The base layered tissue model was used for lifelike simulations. (b) Distance for the tissue layered model vs. the equivalent distance in the experimental model.

via an earpiece with the handset carried near the testicular region. Overall, the study showed that the electromagnetic signals emitted by a cell phone can penetrate the testicular tissues and reach the spermatozoa contained in the seminiferous tubules inside the testis when the cell phone is placed nearby during a call. However, the amount of energy absorbed in that region was lower than the amount absorbed by a semen sample in a test tube. This decrease in the energy density at the ROI in the lifelike model was due to the testicular tissues that separate the cell phone and the spermatozoa. The permittivities of these tissues were considerably higher than the permittivity of air, so the tissues absorbed more of the energy radiated from the cell phone than the air did. Moreover, the thickness of these tissues caused an increase in the actual distance between the source and ROI.

During experimentation, a similar SAR value could be obtained by placing the cell phone a few centimeters farther away from the semen sample than the location of the actual phone in the life-like model. The difference in distance that must be considered to equalize the two settings ranged from about 0.8 cm to 1.8 cm. As depicted in Fig. 3, this difference became larger as the source was placed farther away from the layers where the energy density was reaching a steady state in the ROI (in a steady state energy density, changing the distance had no more effect on the energy density values). For example, if the phone antenna was 1.5 cm away from the reproductive organs in an average male human, the phone antenna should be positioned 2.5 cm from the testing tube to represent a similar effect (Fig. 3b). This relationship suggests that the effect on fertility found in the in vitro study performed by Agarwal et al. (2008, 2009), where the phone was placed 2.5 cm away from the testing tube, would be similar if the phone was placed 1.5 cm from the male's reproductive organs in real life. Fig. 3 also provides guidelines for the equivalent distances that must be considered when performing an in vitro experiment to mimic real life conditions.

The results shown in Table 2 illustrate how the energy density, u, decreases in the ROI as the tissues thicken. The model tested with the thickest range of tissue layers showed a 22% lower mean value of u at the ROI than the model with the thinnest layers. The difference between the distance in the lifelike model and its

equivalent distance in the experimental model was increased from 0.8 cm for the thinnest model to 1.8 cm for the thickest model (Table 2). Thus, the energy density results are sensitive to tissue thicknesses. The authors advise that before performing an in vitro experiment, the measurements of the tissue thicknesses of the subject should be noted or the distances corresponding to the tissue thicknesses for an average male human should be considered, as in the base model considered for this study.

In both setup conditions, the models tested at 1,800 MHz frequency were about 24% higher in energy density, *u*, than the corresponding models at 900 MHz when the source was 2.5 cm from the outermost layer, and 20% higher when the source was 3.5 cm from the outermost layer. These results are congruent with the findings of Flyckt et al. (2007), Martínez-Búrdalo et al. (2001), and Dimbylow (1993) who reported higher SAR values in the head and eye regions at 1,800 MHz than at 900 MHz. Despite the increase in energy density in the 1,800 MHz models, the distance relationship between the lifelike model and the experimental model remained the same for both frequency bands.

It was found that the closest match to the tissue layered model that had the source 2.5 cm from the outer tissue layer was the experimental model that had the source approximately 3.3 cm from the test tube layer for both the 900 MHz and the 1,800 MHz bands. This suggests that the same range of equivalent distances provided in Fig. 3 for the models at 900 MHz can also be used for a source operating at 1,800 MHz. Furthermore, the energy density values became higher as the source size became smaller, as indicated from the analysis that used the point source (Fig. 4). The radiated energy from the current source was distributed along the source so the power and energy were more scattered in the surrounding area. This resulted in a decrease in the energy density as the source size increased, provided that both the ROI and the source were positioned at the center of the x-axis. This difference, however, did not affect the relation of the source-layer separation distance as long as the same source was considered for both settings (Fig. 4), but it agrees with the finding of Mohammed and Hult (2007) and Xiao et al. (2008) that the antenna size and type effect the SAR and energy density. Therefore, the distance guide provided in this study (Fig. 3b) will likely qualify for different antenna sizes and for the 900/1,800 MHz frequency bands, as long as the same source is considered for both the experimental and the lifelike conditions.

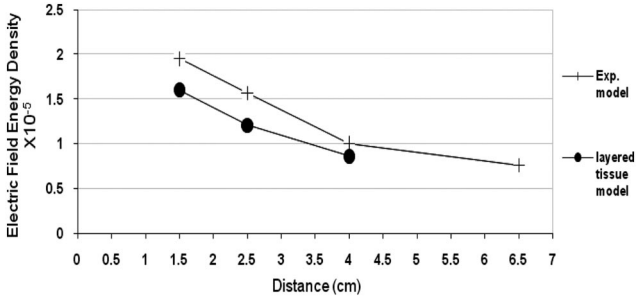

Fig. 4. The average values of the electric field energy density at the ROI for the layered tissue model and for the in vitro experimentation model as a function of distance between the source and outermost region of the model. A 900-MHz point source was used for this simulation. The base layered tissue model was used for lifelike simulations.

Another experimental model was tested after eliminating the test tube layer to examine its effect on the results. The difference in the mean value of the energy density between the two simulations (with and without the test tube) was only 1.5%. From this result, one can infer that the polystyrene test tube did not have a significant effect on the energy density values at the ROI. This was due to the thin walls and low permittivity of the polystyrene test tubes. Therefore, it is likely that the relative relationship between the distances predicted for the experimental and the lifelike models will remain similar if test tubes of other types with similar permittivity and similar wall thickness, such as the standard propylene tubes, were used.

This study has some limitations. A two-dimensional model simulation was used instead of a three-dimensional model. It is possible to develop a complex three-dimensional model representative of intrinsic anatomical details and cell phone characteristics. Such an approach will likely allow one to predict the electric field with an increased accuracy, but the improvement on the precision of comparing different conditions (e.g., anatomical vs. in vivo) may not be dramatic. This work required multiple simulations to be conducted, which may be computationally challenging when three-dimensional models are used. In addition, a three-dimensional model will also require a full anatomical reconstruction, which may not be cost-effective when interest lies in relative changes between conditions. In addition, the lifelike model did not consider the potential additional effects that layers of clothing might have on the results (Chen 2003). Finally, the use of the RF current source in this modeling simulation instead of a cell phone model was another limiting factor. This was thought to be sufficient for comparison purposes as long as the same source was used in both basic modeling conditions.

In conclusion, these results showed that the electromagnetic signals emitted by a cell phone can penetrate testicular tissues when the phone is kept near the groin during a call. This study also establishes a relationship between an in vitro experimental setup and the real life conditions of men when they conduct a cell phone conversation via an earpiece with the handset within a close proximity to their reproductive organs. Simulation using the

Finite Difference Time Domain (FDTD) method demonstrated that the distance between a cell phone and semen sample should be 0.8 cm to 1.8 cm greater than the anticipated distance between the cell phone and testes. The results of this study can be used as the basis to calculate the distance between a radiation source and a semen sample and to set up an in vitro experiment that will mimic real life conditions. This study was the first step in a series of related studies that might follow.

Acknowledgments—The authors would like to thank Reda Mahfouz, from the Center for Reproductive Medicine at Cleveland Clinic Foundation, who helped review the anatomical data for the tissue layered model, and Daniel Simon from the Department of Electrical and Computer Engineering at Cleveland State University for his help in reviewing and commenting on this article.

Research support provided by the Center for Reproductive Medicine, Cleveland Clinic and Research Program Committee (RPC), Cleveland Clinic.

REFERENCES

Agarwal A, Deepinder F, Sharma RK, Ranga G, Li J. Effect of cell phone usage on semen analysis in men attending infertility clinic: an observational study. Fertil Steril 89:124–148; 2008.

Agarwal A, Desai NR, Makker K, Varghese A, Mouradi R, Sabanegh E, Sharma R. Effects of radiofrequency electromagnetic waves (RF-EMW) from cellular phones on human ejaculated semen: an in vitro pilot study. Fertil Steril 92(4): 1318–1325; 2009.

Barnes FS. Bioengineering and biophysical aspects of electromagnetic field: handbook of biological effects of electromagnetic fields. Boca Raton, FL: Taylor & Francis; 2007.

Beard BB, Kainz W. Review and standardization of cell phone exposure calculations using the SAM phantom and anatomically correct head models. Biomed Eng Online 3:34; 2004.

Bit-Babik G, Chou CK, Faraone A, Gessner A, Kanda M, Balzano Q. Estimation of the SAR in the human head and body due to radiofrequency radiation exposure from handheld mobile phones with hands-free accessories. Radiat Res 159:550–557; 2003.

Blank M, Goodman R. A mechanism for stimulation of biosynthesis by electromagnetic fields: charge transfer in DNA and base pair separation. J Cell Physiol 214:20–26; 2008.

Casey R, Jewett MA, Facey RA. Effective depth of spermatogonia in man I. Measurement of scrotal thickness. Phys Med Biol 27:1349–1356; 1982.

Chen H-YS, Kun-Yi. Reduction of SAR in a human-head model wrapped in clothing materials. Microwave Optical Technol Lett 37:305–308; 2003.

Christ A, Samaras T, Klingenbock A, Kuster N. Characterization of the electromagnetic near-field absorption in layered biological tissue in the frequency range from 30 MHz to 6,000 MHz. Phys Med Biol 51:4951–4965; 2006.

Clemente C. Gray's anatomy of the human body. Baltimore: Lippincott Williams & Wilkins; 1985.

Copenhaver WM. Bailey's textbook of histology. Baltimore, MD; Williams & Wilkins; 1978.

Davoudi M, Brossner C, Kuber W. The influence of electromagnetic waves on sperm motility. Urol Urogynacol 19: 18–32; 2002.

Dimbylow PJ. FDTD calculations of the SAR for a dipole closely coupled to the head at 900 MHz and 1.9 GHz. Phys Med Biol 38:361–368; 1993.

Dogra VS, Gottlieb RH, Oka M, Rubens DJ. Sonography of the scrotum. Radiol 227:18–36; 2003.

Farjadpour A, Roundy D, Rodriguez A, Ibanescu M, Bermel P, Joannopoulos JD, Johnson SG, Burr GW. Improving accuracy by subpixel smoothing in the finite-difference time domain. Opt Lett 31:2972–2974; 2006.

Fejes I, Zavaczki Z, Szollosi J, Koloszar S, Daru J, Kovacs L, Pal A. Is there a relationship between cell phone use and semen quality? Arch Androl 51:385–393; 2005.

Flyckt VM, Raaymakers BW, Kroeze H, Lagendijk JJ. Calculation of SAR and temperature rise in a high-resolution vascularized model of the human eye and orbit when exposed to a dipole antenna at 900, 1500 and 1800 MHz. Phys Med Biol 52:2691–2701; 2007.

Gabriel S, Lau RW, Gabriel C. The dielectric properties of biological tissues: II. Measurements in the frequency range 10 Hz to 20 GHz. Phys Med Biol 41:2251–2269; 1996.

Gajsek P, Ziriax JM, Hurt WD, Walters TJ, Mason PA. Predicted SAR in Sprague-Dawley rat as a function of permittivity values. Bioelectromagnetics 22:384–400; 2001.

Karygiannis T, Owens L. Wireless Network Security 802.11. Bluetooth and handheld devices. Gaithersburg, MD: National Institute of Standards and Technology; 2002: 800–848.

Laakso I, Ilvonen S, Uusitupa T. Performance of convolutional PML absorbing boundary conditions in finite-difference time-domain SAR calculations. Phys Med Biol 52:7183–7192; 2007.

Makker K, Varghese A, Desai NR, Mouradi R, Agarwal A. Cell phones: modern man's nemesis? Reprod Biomed Online 18:148–157; 2009.

Martínez-Búrdalo M, Nonidez L, Martín A, Villar R. FDTD analysis of the maximum SAR when operating a mobile phone near a human eye and a wall. Microwave and Optical Technol Lett 28:83–85; 2001.

Mohammed A, Hult T. The effects of MIMO antenna system parameters and carrier frequency on active control suppression of EM fields. Radioengineering 16:31–35; 2007.

Standring S. Gray's anatomy: the anatomical basis of clinical practice; 39th ed. New York: Churchill Livingstone; 2004.

Taflove A. Computational electrodynamics, the Finite-Difference Time-Domain Method. Artech House: Norwood, MA; 2005.

Tretyakov SA. Electromagnetic field energy density in artificial microwave materials with strong dispersion and loss. Phys Letters A 343(1–3):231–237; 2005.

Wdowiak A, Wdowiak L, Wiktor H. Evaluation of the effect of using mobile phones on male fertility. Ann Agric Environ Med 14:169–172; 2007.

Xiao SCJ, Liu X, Wang B-Z. Spatial focusing characteristics of time reversal UWB pulse transmission with different antenna arrays. Progress Electromagnetics Research 2:223–232; 2008.

Yang WQ. Calibration of capacitance tomography systems: a new method for setting system measurement range. Meas Sci Technol 7(6):L863–L867; 1996.

World Health Organization. 2006 WHO research agenda for radio frequency fields. 2006. Available at http://www.who.int/peh-emf/research/rf_research_agenda_2006.pdf. Accessed 29 October 2011.

■ ■